International Journal of Biological Macromolecules 59 (2013) 227–234

Contents lists available at SciVerse ScienceDirect

International Journal of Biological Macromolecules

journal homepage: www.elsevier.com/locate/ijbiomac

Preparation and properties of g-TTCP/PBS nanocomposites and its *in vitro* biocompatibility assay

Rang Rang Fan[a], Liang Xue Zhou[a,1], Wei Song[b], De Xia Li[a], Dong Mei Zhang[a], Rui Ye[a], Yu Zheng[a], Gang Guo[a,*]

[a] State Key Laboratory of Biotherapy and Cancer Center, Department of Neurosurgery, West China Hospital, West China Medical School, Sichuan University, Chengdu 610041, PR China
[b] Institute of Biochemistry and Cell biology, Shanghai Institutes for Biological Sciences, CAS, Shanghai 200031, PR China

ARTICLE INFO

Article history:
Received 26 February 2013
Received in revised form 7 April 2013
Accepted 16 April 2013
Available online 23 April 2013

Keywords:
Surface grafting
Tetracalcium phosphate
Poly(butylene succinate)
Osteoblasts

ABSTRACT

In an effort to decrease the aggregation of tetracalcium phosphate (TTCP, $Ca_4(PO_4)_2O$) in composites and develop better bone substitute materials, a series of poly(L-lactic acid) (PLLA)-grafted TTCP (g-TTCP) particles were prepared by a ring-opening polymerization with L-lactide (the monomer for synthesizing PLLA) in the presence of catalyst stannous octoate [$Sn(Oct)_2$]. The g-TTCP/poly(1,4-butylene succinate) (PBS) composites with the different g-TTCP contents were prepared *via* melting processing. The bonding between the PLLA and the TTCP particles was analyzed by FTIR, TG, ^1H NMR and XPS. The results confirmed that the PLLA was grafted on the surface of the TTCP particles. Time-dependent phase monitoring indicated that the g-TTCP had enhanced dispersion in the PBS solution. Water contact angle measurement and cell culture were also used to investigate the properties of the g-TTCP/PBS composites. The g-TTCP in composites provided more favorable environments for rat osteoblast to attach and grow on the surface of the g-TTCP/PBS composites. Cell proliferated well in the extracted solution of the g-TTCP/PBS composites with different g-TTCP content, and there was no necrotic or suspended cells appeared.

1. Introduction

In the past several decades, many efforts have been made toward to synthesize the new bone substitute materials [1–3]. Among these, inorganic–polymer nanocomposites have attracted much attention because of their unique combination of properties and widespread potential applications in bone tissue engineering [4–7]. And the combination of calcium phosphates with polymers had been the subject of numerous investigations because of the same ions as the mineral in natural bone [8–12]. Hydroxyapatite (HA, $Ca_{10}(PO_4)_6(OH)_2$), tetracalcium phosphate (TTCP, $Ca_4(PO_4)_2O$), tricalcium phosphate (β-TCP, $Ca_3(PO_4)_2$) and their composites are highly attractive for many clinical uses due to, among other reasons, their excellent tissue response, bioresorption and osteoconductivity [13–16].

The interfacial strength between nanoparticle and polymer is a key factor associated with the construction of nanocomposites. However, the tendency for agglomeration makes it very difficult to process nanocomposites with a high degree of particle dispersion [17]. Particle aggregates in composite materials tend to decrease adhesion between the two phases which will result in an early failure at the interface and thus increases the susceptibility to physical and mechanical failure especially in terms of tensile strength [18]. Much attention has been paid to improve the interfacial adhesion between the calcium phosphate particles and polymer matrix [19]. The surface of calcium phosphate crystals has been modified by a series of coupling agents and polymers through the chemical reaction with hydroxyl groups on the calcium phosphate particles [20–22]. And the affinity of the particle surface to the polymer matrix was improved to some extent. Thus, surface functionalization of TTCP may play a significant role in producing well-dispersed TTCP/polymer composites.

Synthetic biodegradable polymers are widely used in bone tissue engineering because they allow new bone mass to substitute various biological functions without potential chronic problems [23–27]. Poly(1,4-butylene succinate) (PBS) is a biodegradable aliphatic polyester synthesized by the condensation polymerization of 1,4-butane diol and succinic acid [28]. It has better processability compared to poly(lactic acid) and poly(glycolic acid) which can be tailored by a variety of fabrication methods to achieve the desired internal architecture [29]. PBS is also proven to possess superior mechanical properties that are comparable to

* Corresponding author at: State Key Laboratory of Biotherapy and Cancer Center, Department of Neurosurgery, West China Hospital, West China Medical School, Sichuan University, Chengdu 610041, PR China. Tel.: +86 2885164063; fax: +86 2885164060.
E-mail address: guogang@scu.edu.cn (G. Guo).
[1] Zhou did the even work with Fan, and is the co-first author for this work.

0141-8130/$ – see front matter © 2013 Elsevier B.V. All rights reserved.
http://dx.doi.org/10.1016/j.ijbiomac.2013.04.051

those of polyethylene and polypropylene [30], which can meet the mechanical requirements of bone tissue engineering. It has been demonstrated to be biocompatible with osteoblasts, due to its ability in supporting both the proliferation and the differentiation of the cells [31–33].

In our previous work, we prepared g-TTCP/PBS nanocomposites by melt processing. The nanocomposites might be potentially used in the field of tissue engineering. In order to investigate the effects of reaction time on the percent grafting and grafting efficiency of PLLA on TTCP surfaces and the *in vitro* biocompatibility of nanocomposites, in this study, a systematic study to control the reactivity of surface hydroxyl groups of TTCP was reported. And we studied the bonding between the PLLA and the TTCP particles by FTIR, XPS and TG-FTIR. The enhanced colloidal stability of g-TTCP in organic solutions was described. We are also interested in knowing whether the presence of g-TTCP displays a positive effect on the cell adhesion and proliferation of g-TTCP/PBS composites.

2. Experimental

2.1. Materials

L-lactide was obtained from Guangshui National Chemical Co. (China). Tetracalcium phosphate (TTCP) was purchased from Ensail Beijing Co., Ltd. (China), with the particle size about 500–800 nm in diameter. Poly(butylene succinate) (PBS), with the relative density of 1.26, was obtained from Anqing He Xing Chemical Corp. Ltd. (China). Stannous octoate ($Sn(Oct)_2$) was obtained from Aldrich (USA); Dulbecco's Modified Eagle Medium (DMEM, the culture medium) and MTT (3-(4,5-dimethylthiazolyl-2)-2,5-diphenyl tetrazolium bromide) were supplied by Sigma (USA). All other agents like methylbenzene, petroleum ether, dichloromethane (CH_2Cl_2) and dimethyl sulfoxide were all of analytical reagent (AR) grade and used as received without further purification.

The osteoblasts used in this study were the immortalized rat osteoblastic ROS 17/2.8 cell line, which obtained from the National Engineering Research Center for Biomaterials, Sichuan University.

2.2. Preparation of PLLA-grafted TTCP by ring-opening polymerization

The grafting polymerization of the PLLA onto the hydroxyl groups through a ring-opening polymerization reaction was briefly described as follows: 1 g TTCP powders which were dried at 135 °C for 8 h, were dispersed in 60 ml methylbenzene under ultrasonication for 10 min at room temperature and 20 g L-lactide was slowly added under stirring, and then the mixture and 0.105 g $Sn(Oct)_2$ were slowly added into the reaction vessel under a nitrogen atmosphere. Then the reaction vessel was placed in an oil bath at 140 °C under nitrogen atmosphere for 2 h, 4 h, 6 h, 12 h, respectively. The reaction mixtures were cooled down to room temperature, precipitated in excess cold petroleum ether. The product was filtered and dried to constant weight at 40 °C in vacuum.

The Soxhlet extractor was used to remove any non-graft PLLA on the surface of TTCP particles using CH_2Cl_2 as solvent at 50 °C for 24 h. The purified g-TTCP was dried to constant weight at 40 °C in vacuum. The extraction solution was centrifugated at 13,000 rpm for 10 min and then PLLA was collected by precipitating the centrifugation solution with methanol. Refined polymer was then dried in vacuum at 40 °C for 24 h and kept in desiccation for further study.

The composites with various amounts (5, 10, 20, and 40 wt.%) of the g-TTCP (12 h) and the pure PBS were prepared in a Haake MiniLab co-rotating twin-screw extruder CTW5 (Thermo Science, Germany) at 180 °C and a rotor speed of 32 rpm. All the resulting composites were injection molded using a Haake Mini Jet machine (Thermo Science, Germany) to produce dumbbell-shaped tensile test bars according to ISO 3167 (2002).

2.3. Transmission electron microscopy (TEM)

TEM was used to examine the microscopy morphology of the TTCP powder by a HITACHI H-600 Electronic Microscopy operating at 100 kV. The samples were dispersed in ethanol to form a suspension by ultrasonication for 60 min and then a drop of suspension was then directly dripped on a copper TEM grid and dried on filter.

2.4. Fourier transform infrared absorption spectra (FT-IR)

FT-IR spectra were used to characterize the chemical structure of pure TTCP, g-TTCP and PLLA on a Nicolet 6700 FT-IR spectrometer (Thermo Science, USA) in a wavenumber range of 4000–400 cm^{-1}. The pure TTCP and g-TTCP powders were mixed with KBr powder and pressed into a pellet. In order to obtain the spectra of PLLA alone, the PLLA was dissolved in dichloromethane and cast onto a KBr plate to form a thin film.

2.5. Nuclear magnetic resonance characterization (^1H NMR)

To compare the chemical composition and molecular structure of the TTCP and the surface-modified TTCP, ^1H NMR spectroscopy were recorded on a Varian 400 instrument (Varian, USA) at 400 MHz using deuterated chloroform ($CDCl_3$) as the solvent, and tetramethylsilane (TMS) was used as an internal reference standard.

2.6. Thermogravimetric analysis

Thermogravimetric analysis (TGA) was performed from room temperature to 600 °C using a TGA Q 500 series Thermogravimetric analyzer (TA Instrument, USA) with a heating rate of 10 °C/min in a nitrogen environment.

2.7. Time-dependent phase monitoring

The TTCP and the PLLA-grafted TTCP (12 h) were added in dichloromethane: chloroform (2:1) solution of PBS (5 wt.%, 1 ml). The mixture was equilibrated by vortex for 15 min and sonicate for 30 min. Phase behavior of each solution mixture was monitored at room temperature as a function of time.

2.8. X-ray photoelectron spectroscopy (XPS)

X-ray photoelectron spectroscopy (XPS) is an ideal instrument for the surface analysis of chemical change as a result of PLLA grafted onto the TTCP surface due to its high sensitivity and non-destructive nature. XPS (Kratos XSAM-800, UK) analyses were conducted by employing Mg Kα X-radiation (1253.6 eV). The binding energy was referenced with respect to the 284.5 eV to the C 1s peak. Experimental data were deconvolved by fitting a mixed Gaussian–Lorentzian function.

2.9. Water contact angle measurement

Water contact angles indicating the wetting ability of g-TTCP/PBS composites were measured by drop shape analysis (DSA 100, KRü SS, Germany) at room temperature. A drop of 3 μl deionized water was dropped on the sample surfaces. At least three measurements were performed at different locations and the

results averaged. The drops were photographed immediately, and the contact angle values can then be calculated from Eq. (1) [34]:

$$\theta = 2\arctan\frac{2h}{b} \quad (1)$$

in which θ is the contact angle, h is the droplet height, and b is half of the droplet width.

2.10. X-ray diffraction measurement

XRD patterns were recorded on a Philips X'Pert PRO XRD meter (Netherlands) with Cu K_α radiation (λ = 0.1542 nm; 40 kV; 40 mA). Data were collected from 10 to 60° with the scanning speed of 0.4° s^{-1}.

2.11. Cell adhesion and proliferation studies

To investigate the immortalized rat osteoblastic ROS 17/2.8 cell morphology of attaching and growing on the surface of g-TTCP/PBS composites, the pure PBS and g-TTCP/PBS specimens containing 5, 10, 20 and 40 wt.% g-TTCP were placed in the bottom of each well of a 24-well culture plate and then sterilized with ethylene oxide (ETO) steam for 24 h at room temperature. Osteoblasts were then seeded onto the surfaces of composites and cultured with Dulbecco's modified Eagle's medium (DMEM) at 37 °C in a 5% CO_2 humidified atmosphere. After incubated for 2 h, 4 h and 6 h, the medium was taken out of the culture plates and the scaffolds were washed with phosphate-buffered saline three times. Then the samples were fixed with 2.5% glutaraldehyde in phosphate-buffered saline for 24 h at 4 °C. After that, the samples were rinsed and dehydrated in ethanol solutions of varying concentrations (*i.e.* 30, 50, 70, 80, 90, 95 and 100%, respectively). Samples were dehydrated twice in each ethanol for 10 min each time.

Cell attachment efficiency on g-TTCP/PBS composite specimens containing 0 and 20 wt.% g-TTCP was measured by MTT (3-(4,5-dimethylthiazol-2-yl)-2,5-diphenyltetrazolium bromide) assay. Briefly, the samples (the pure PBS and g-TTCP/PBS specimens containing 20 wt.% g-TTCP) were fixed in each bottom of a 24-well cell culture plate and sterilized with ethylene oxide (ETO) steam for 24 h at room temperature. 1 ml DMEM was added into each well, respectively. The cell culture was maintained in a 37 °C incubator with a humidified 5% CO_2 atmosphere, then 1 ml cell suspension (about 5×10^4 cells) was seeded evenly in each well. And the cells without a scaffold served as the negative control. After seeding for 1, 3, and 5 days, 100 μl of MTT (5 mg/mL) solution was added to each well and incubated at 37 °C for 4 h, respectively; after removing supernatants, 800 μl of DMSO was added to each well for dissolving the blue formazan crystal. Finally, the solution (150 μl) was collected and transferred into a 96-well plate. The absorbance of each well was recorded on an ELISA microplate reader (Bio-Rad, USA) at 570 nm. A mean value was obtained from the measurement of four test runs.

Modified MTT assay was applied to analysis the cell proliferation in the extracted solution of the g-TTCP/PBS composites with different g-TTCP content (the pure PBS and g-TTCP/PBS specimens containing 5, 10, 20 and 40 wt.%). The method was similar as which was described above. The cell culture was maintained in a 37 °C incubator with a humidified 5% CO_2 atmosphere for 1 day. The extract was transferred to new 24-well culture plate. Then 1 ml cell suspension (about 5×10^4 cells) was seeded evenly in each well. And the cells without a scaffold served as the negative control. The cell culture was maintained in a 37 °C incubator with a humidified 5% CO_2 atmosphere for 1, 3 and 5 days. The absorbance of each well was recorded on an ELISA microplate reader (Bio-Rad, USA) at 570 nm. A mean value was obtained from the measurement of four test runs.

Fig. 1. TEM photographs of TTCP powder.

3. Results

3.1. Preparation and characterization of PLLA-grafted TTCP

Scheme 1 showed the process of synthesizing of the g-TTCP. TEM photographs of TTCP crystals were presented in Fig. 1. And the FTIR spectra of the pure PLLA, the bare TTCP and the g-TTCP are presented in Fig. 2. In the spectrum of the g-TTCP, the new bands at 2994.1 and 1759.8 cm^{-1} were attributed to the —CH and the C=O bonds vibration. A broad peaks at 3300–3500 cm^{-1} was related to the OH— from the PLLA and the absorbed water, and the peaks at 1094.4, 1064.4 and 1011.9 cm^{-1} were attributed to v_3-P-O vibrations of phosphate groups (PO_4^{3-}); the absorption peaks at 620.6 and 568.4 cm^{-1} corresponded to v_4-P-O vibrations of PO_4^{3-} besides of the above described absorption peaks, there were two weak peaks at 956.4 and 473.7 cm^{-1} which were attributed to v_1 and v_2 vibrations of PO_4^{3-} ions, respectively.

Fig. 3 presented the ^1H NMR spectrums of the PLLA collected from centrifugation solution. The characteristic absorption peaks were also presented in Fig. 2. The chemical shifts of protons with —CH and —CH_3 were 5.17 and 1.57.

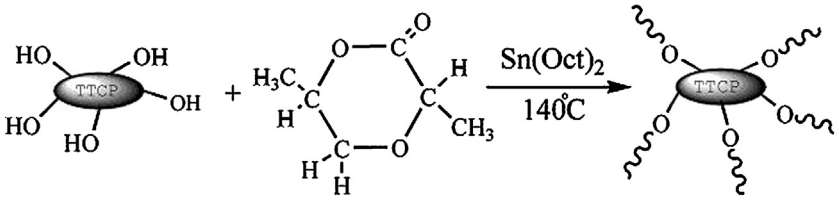

Scheme 1. Synthesis scheme of PLLA grafted TTCP.

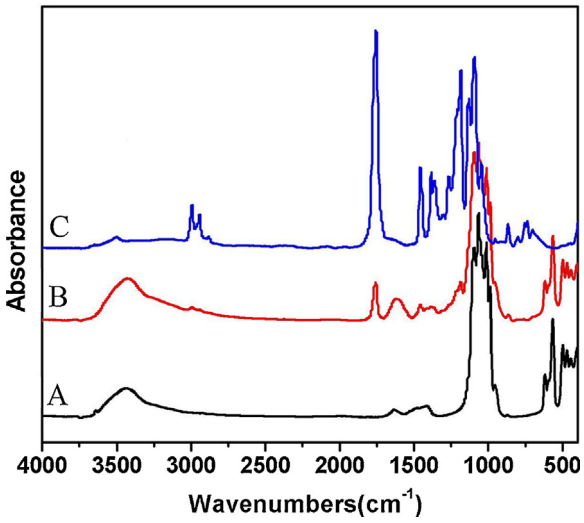

Fig. 2. FTIR spectra for pure TTCP (A), PLLA-grafted TTCP (B) and PLLA (C).

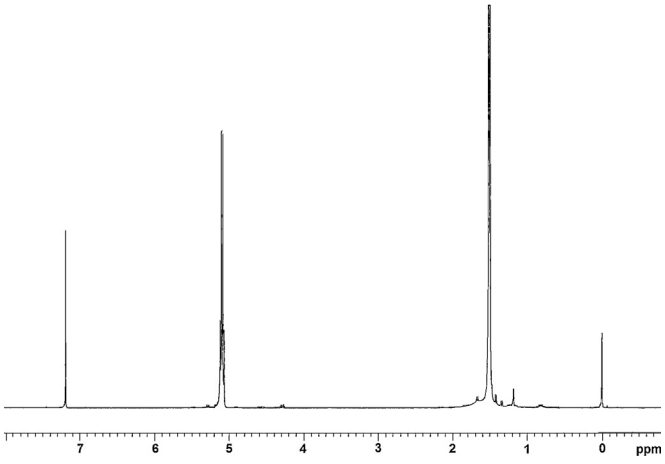

Fig. 3. ^{1}H NMR spectrums of PLLA collected from centrifugation solution.

3.2. TG analysis

Fig. 4 showed TG curves of the pure TTCP, the g-TTCP prepared at different reaction times (2 h, 4 h, 6 h and 12 h). The amount of the surface grafted PLLA was determined as a weight loss percentage during heating. Eqs. (2) and (3) were respectively used to count the percent of PLLA grafted on the TTCP surface and the grafting efficiency [35].

$$\text{grafting percentage}\,(\%) = \frac{\text{grafted PLLA on TTCP}\,(g)}{\text{PLLA} - \text{grafted TTCP}\,(g)} \times 100 \quad (2)$$

$$\text{grafting efficiency}\,(\%) = \frac{\text{grafted PLLA on TTCP}\,(g)}{\text{LA used}\,(g)} \times 100 \quad (3)$$

The grafted PLLA on the TTCP was measured by TGA, and the PLLA used was the feed amount for graft polymerization.

The weight loss of the TTCP, the g-TTCP for 2 h, 4 h, 6 h and 12 h were 0.94%, 7.55%, 8.28%, 10.59% and 21.93%. According to the equation that the grafting amount (%) = $W(\%) - W_0(\%)$, where W is the weight loss of the g-TTCP, and W_0 is the weight loss of the pure TTCP, it can be concluded that the PLLA grafting percentage at 2 h, 4 h, 6 h and 12 h were 6.61%, 7.34%, 9.51% and 20.99%, respectively. The grafting efficiency of the g-TTCP for 2 h, 4 h, 6 h and 12 h were about 5%, 8%, 11% and 15%.

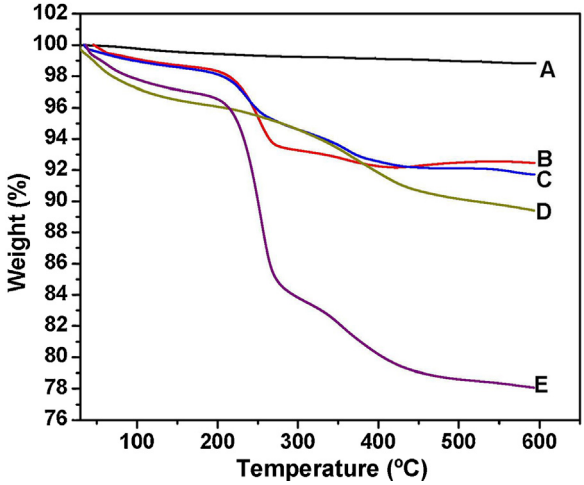

Fig. 4. TG curves of pure TTCP (A), PLLA-grafted TTCP prepared at different reaction times: 2 h (B), 4 h (C), 6 h (D) and 12 h (E).

3.3. Phase behavior of solutions of PBS/TTCP and PBS/PLLA-grafted TTCP

Fig. 5 showed the time-dependent colloidal stability of the PBS/TTCP and the PBS/PLLA-grafted TTCP in a solution (dichloromethane:chloroform = 2:1). It can be seen that the phase separation of solution mixture of the PBS and the untreated TTCP was examined in less than 10 min, however, the colloidal stability of the PLLA-grafted TTCP in solution mixture increased dramatically.

3.4. XPS analysis

Fig. 6 showed the XPS spectra of Ca and O 1s core level spectra of the pure TTCP; Ca and O1s core level spectra of the g-TTCP. The O 1s signal for the TTCP and the g-TTCP were located at binding energy of 531.85, 532.05 eV and 530.50, 531.65 eV, respectively. The XPS spectra of Ca for the TTCP and the g-TTCP were found at binding energies of 347.00, 350.70 eV and 346.85, 350.43 eV.

3.5. Contact angle analysis

Fig. 7 showed the surface wettability of the g-TTCP/PBS composites with different g-TTCP contents. It can be seen that the water contact angles of all composites were less than 90° which indicated that these composites were hydrophilic in some extent; the contact angle value of pure PBS was 62.6 ± 0.7°. The contact angles of the g-TTCP/PBS composites tended to increase with the increase of g-TTCP content, and the composites had the largest value at 74.5 ± 1.3° as g-TTCP content increased to 40 wt.%; when adding 10 wt.% g-TTCP into PBS, the value decreased to 66.0 ± 0.8°, it was less than that of the g-TTCP/PBS composite containing 5 wt.% g-TTCP but still was higher than that of the pure PBS.

3.6. XRD characterization

Fig. 8 showed the XRD patterns of the pure TTCP (A), the g-TTCP (B) and the PLLA (C). In the pattern of the pure TTCP, the obvious peaks were observed at 2θ = 21.82, 25.42, 29.86, 32.41. And the g-TTCP has several major peaks at 2θ = 21.85, 25.54, 29.98, 32.56.

3.7. Cell adhesion and proliferation analysis

In this study, ROS 17/2.8 cells were used as a model to compare cellular morphology of attaching and growing on the surface

Fig. 5. Time-dependent colloidal stability of the mixture of PBS/TTCP and PBS/PLLA-grafted TTCP: A 0 min; B 10 min; C 60 min.

of scaffolds with and without the g-TTCP. The cell state and attaching behavior were observed by SEM (JSM-7500F, JEOL, Japan) and shown in Fig. 9(a). The cells on the surface of composite scaffolds spreaded well and their morphology was satisfactory. Some cells had spread and their pseudopodia had grown. Fig. 9(b) showed the cell attachment efficiency on g-TTCP/PBS composite specimens containing 0 and 20 wt.% g-TTCP measured by MTT assay.

The cell viability of osteoblasts on the different composites using MTT assay is shown in Fig. 10. The osteoblasts were cultured in the extract of the g-TTCP/PBS composites for 1, 3 and 5 days, respectively. It can be seen from Fig. 10 that the osteoblasts proliferated with the culture time on all the composites of the g-TTCP/PBS and the pure PBS. The results showed that the osteoblasts proliferated rapidly after seeding for 3 days; and they increased approximately triple during 5 days in culture.

4. Discussion

Tissue engineering, a promising approach to repair damaged tissues/organs has developed rapidly in recent years. Development

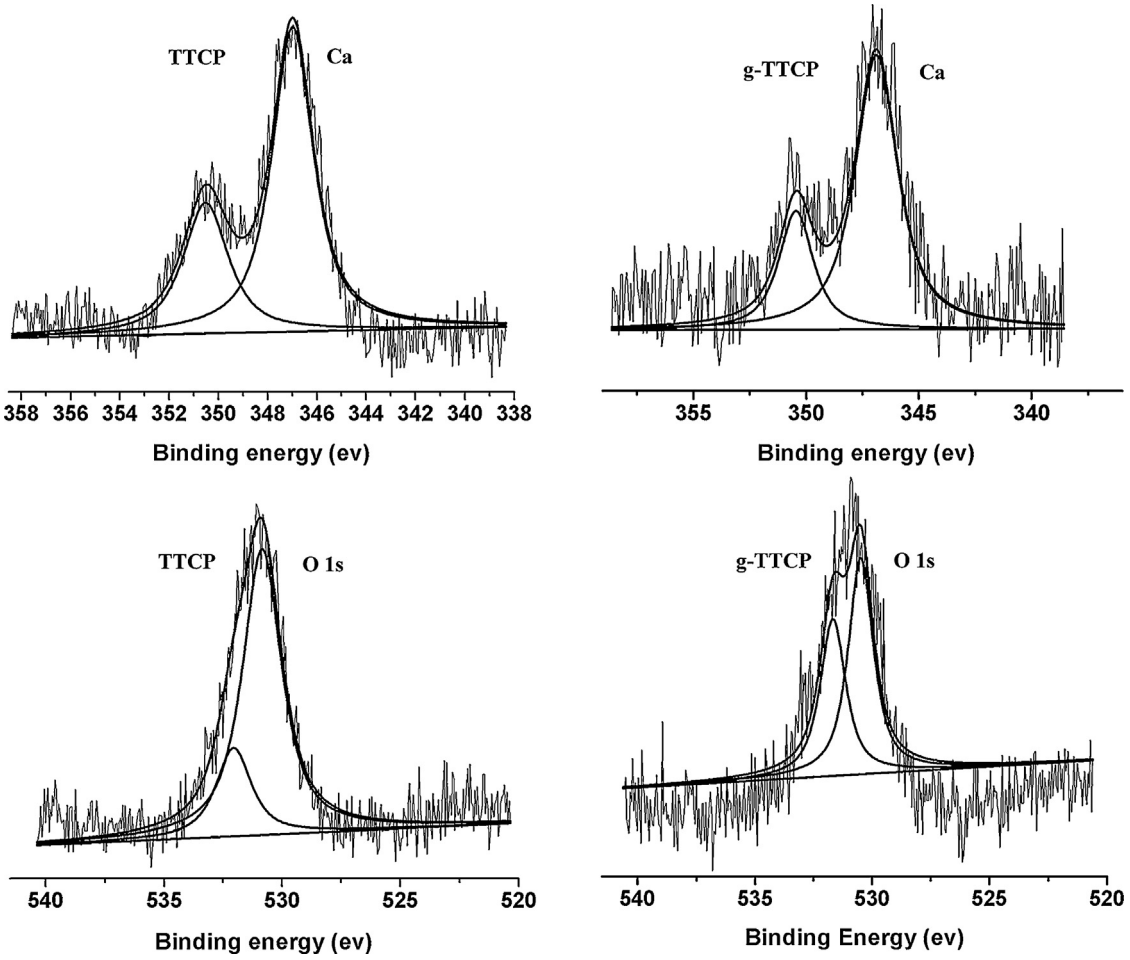

Fig. 6. XPS spectra of Ca and O 1s of the pure TTCP and PLLA-grafted TTCP.

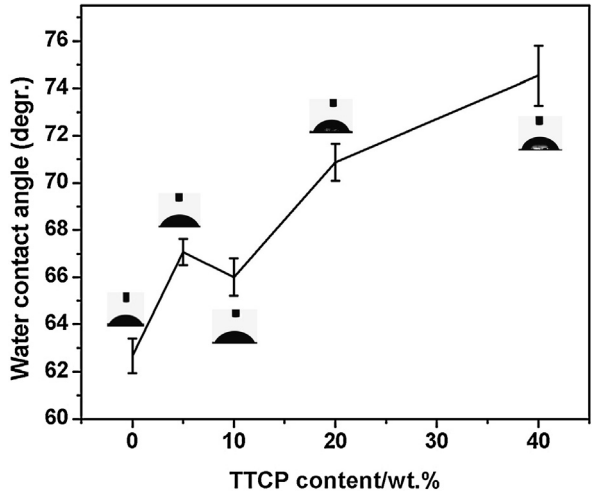

Fig. 7. Water contact angles of the g-TTCP/PBS composites.

of biomaterials suitable for cell attachment, proliferation and differentiation opens avenues to engineering vital and transplantable tissues and organs for research and clinical application [36,37]. Ceramic/polymer composites have gained much recognition as bone scaffolds because of their structural and compositional similarities to natural bone and their unique functional properties [7,38]. And most surface modification work has been done on n-HA and TCP, the reactions of which have been extensively characterized and well understood [12,15]. However, there is no literature about TTCP used in surface modification for composite scaffold according to our knowledge. In this study, the PLLA-grafted TTCP particles were prepared by ring-opening polymerization of L-lactide onto the surface of the TTCP particles. A series of the g-TTCP/PBS composites with different the g-TTCP contents were prepared *via* melting processing. Mechanical properties have been studied in our previous work, the results revealed that the tensile strengths of the composites containing 10 wt.% of g-TTCP was the greatest, which was 25% higher than that of PBS alone. This suggested that the nanocomposites might be potentially used in the field of tissue engineering. So we studied the cytocompatibility of composites for cell adhesion and proliferation using osteoblast cells in the present study.

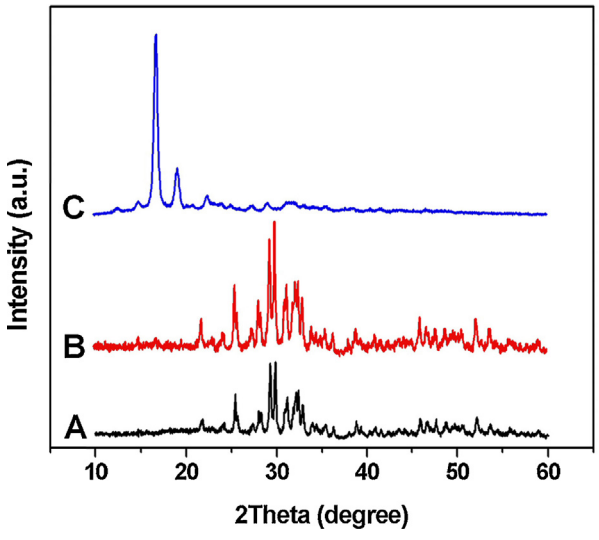

Fig. 8. XRD patterns of TTCP (A), g-TTCP (B), and PLLA (C).

FTIR and ^{1}H NMR were used to characterize the bonding between the PLLA and the TTCP particles, from the results of FTIR analysis as shown in Fig. 2, the characteristic band of carbonyl groups at 2994.9 cm^{-1} and 1759.8 cm^{-1} confirmed the formation of the g-TTCP. According to the integral intensities of characteristic absorption peaks in Fig. 3, the M_n of the PLLA was calculated to be 1000, which was slightly smaller than the theoretical value of 1200 based on feed ratio.

The amounts of the grafted PLLA on the surface of the TTCP were measured by TGA. The plots provide the information about the time-depended grafting amount of the PLLA on the TTCP. The weight loss of the inorganic TTCP was 0.94% up to 600 °C, thus we can conclude that the weight loss is exclusively attributed to the organic substances of the grafted PLLA. The grafting amount of the PLLA at a reaction time of 2 h was 6.61%, and gradually increased as the reaction time increased. The 20.99% PLLA was grafted on the surface of the TTCP at a reaction time of 12 h.

The monitoring of time-dependent colloidal stability of the unmodified TTCP and the g-TTCP was showed in Fig. 5. The colloidal stability dramatically increased when the PLLA was grafted on to the surface of the TTCP. This phase behavior was ascribed to the enhanced colloidal stability of the g-TTCP in the poly(1,4-butylene succinate) solution. On the basis of the preliminary study, we confirmed that g-TTCP showing the good dispersibility in solutions could serve as an excellent adhesion enhancer between organic PBS phases and inorganic TTCP phases.

X-ray photoelectron spectroscopy (XPS) is an ideal instrument to analyze the surface chemical compositions of the TTCP and the g-TTCP due to its high sensitivity. The XPS spectra of Ca and O 1s core level spectra of the pure TTCP and the g-TTCP were showed in Fig. 6. Peaks corresponding to $Ca2p_{3/2}$ (347.00 eV), $Ca2p_{1/2}$ (350.70 eV) of TTCP and $Ca2p_{3/2}$ (346.85 eV), $Ca2p_{1/2}$ (350.43 eV) of g-TTCP were clearly observed. Only a slight shift toward low binding energies was found when observing the Ca 2p line. For the pure TTCP, the bonding energies of 531.85 eV and 532.05 eV were because of OH— and PO_4^{3-} species on the surface. The O 1s binding energies decreased when PLLA was grafted onto the surface of the TTCP. This may be correlated to the contributions from the polymer in C═O, C—O groups.

The surface wettabilities of all composites were determined by water contact angle measurements. The contact angle values were less than 90° indicating that all scaffolds were hydrophilic. As the g-TTCP loadings increased, the values also increased. The reason for this may be the increase of the PLLA content and the rougher surface of the g-TTCP/PBS composites compared to that of the pure PBS which might prevent the water drop penetrating into the pores and hollows. The g-TTCP is intrinsically hydrophobic material, so the addition of the g-TTCP into the PBS matrix decreased the hydrophilicity of the PBS.

The pure TTCP in Fig. 8 had several major characteristic peaks at angles of $2\theta = 21.82, 25.42, 29.86, 32.41$ for its regular crystallization [39]. The pattern of the g-TTCP indicated that the PLLA grafted-TTCP still kept the typical crystallinity.

The cell adhesion is an important cellular process to examine the influence of the biocompatible scaffold on cell proliferation and osteogenesis. In general, cellular interaction with bioactive material surface reflects the biological behaviors of the biomaterials [40,41]. In order to investigate the cell adhesion and viability on the surface of the g-TTCP/PBS composites, the osteoblasts morphology of the samples were examined 4 h, 6 h and 8 h post-seeding. Just as shown in Fig. 9, the osteoblasts on the surface of composites displayed good attachment behavior. It revealed that the g-TTCP/PBS composites could provide a suitable environment for cell attachment and proliferation. The cell viabilities measured by MTT assay in the extracted solution of the g-TTCP/PBS

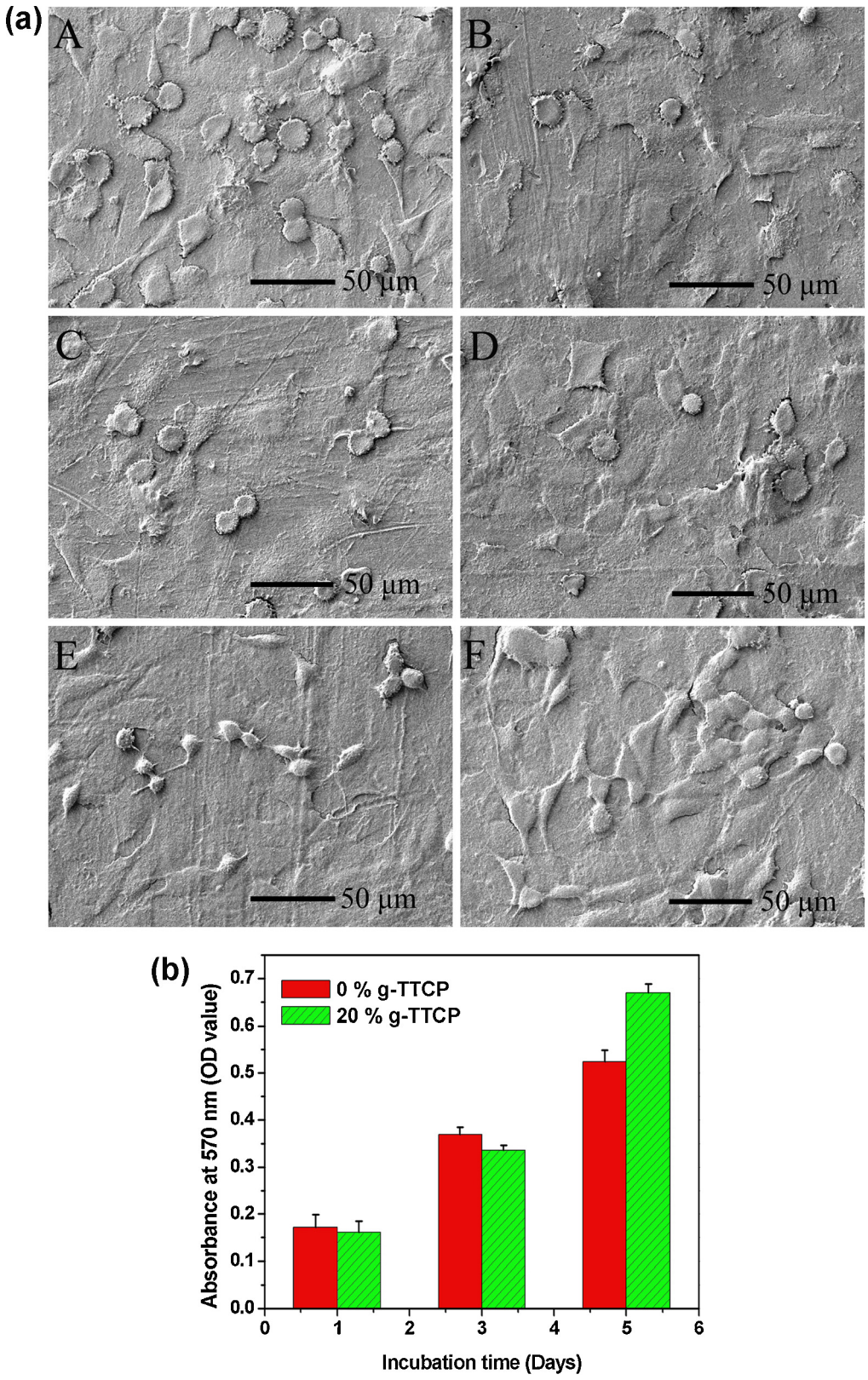

Fig. 9. (a) SEM observations of osteoblast cell adhesion and growth on pure PBS specimen (A, C, E) and the g-TTCP/PBS composite specimens containing 20 wt.% grafted TTCP (B, D, F); A, B, cultured for 2 h, C, D, cultured for 4 h, E, F cultured for 6 h. (b) Cell attachment efficiency on g-TTCP/PBS composite specimens containing 0 and 20 wt.%.

composites for 1, 3 and 5 days were shown in Fig. 10 ("embed Figure 10"). From the MTT data, we can see that all the samples got the upward trend, suggesting that osteoblasts could grow in the extracted solution of the g-TTCP/PBS composites. As clearly shown in Fig. 10, the osteoblasts proliferated significantly when the weight ratio of the g-TTCP to PBS was 10 wt.%. The cell adhesion and proliferation behavior suggested that the g-TTCP/PBS composites had good biocompatibility and could be one of the

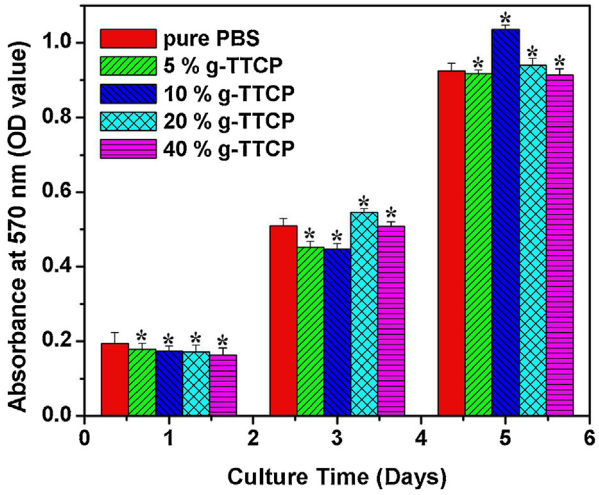

Fig. 10. MTT assays for cell proliferation of osteoblast cell cultured on PBS and g-TTCP/PBS composite scaffolds of different g-TTCP content cultured for 1, 3, and 5 days. Data were expressed as means ± standard deviation (SD). Significant at the $^{*}p < 0.05$ level when pure PBS was the control.

best potential bone implant candidates in bone tissue engineering.

4.1. Conclusion

The TTCP particles have been successfully modified with L-lactide *via* ring-opening polymerization reaction on their surface. Melt blending was used to prepare g-TTCP/PBS composites. The modified TTCP has good dispersibility and improved interfacial interactions. The addition of the g-TTCP in the PBS can effectively improve the hydrophobic property of the PBS. Osteoblast culturing and MTT assays showed that the composites had good biocompatibility in terms of osteoblast attachment, spreading and proliferation on the composites. In further studies, the PBS scaffold blend or chemical modification with other polymers should be studied. More research is need to validate the application of these composites, possibly by investigating them with osteoblasts and growth factors *in vitro* and *in vivo*, in particular animal tests to find clinical applications such as guided bone regeneration and tissue engineering matrices.

Acknowledgements

This work was financially supported by Youth Foundation of Sichuan University (2008103) and the National S&T Major Project (2011ZX09102-001-10). The authors thank Wang Hui and Chen Hong (Analytical & Testing Center, Sichuan University) for their separate help in SEM observation and XPS analysis.

References

[1] A.A. Deschamps, M.B. Claase, W.J. Sleijster, J.D. de Bruijn, D.W. Grijpma, J. Feijen, Journal of Controlled Release 78 (2002) 175–186.
[2] K. Sahithi, M. Swetha, K. Ramasamy, N. Srinivasan, International Journal of Biological Macromolecules 46 (2010) 281–283.
[3] F. Variola, J.B. Brunski, G. Orsini, P. Tambasco de Oliveira, R. Wazen, A. Nanci, Nanoscale 3 (2011) 335–353.
[4] S. Wei, Q. Wang, J. Zhu, L. Sun, H. Lin, Z. Guo, Nanoscale 3 (2011) 4474–4502.
[5] G. Guo, J. Yu, Z. Luo, Z.Y. Qian, W.X. Huang, M.J. Tu, Acta Pharmacologica Sinica 6 (2006) 219–224.
[6] G. Guo, J. Yu, Z. Luo, L.X. Zhou, H. Liang, F. Luo, Z.Y. Qian, Journal of Nanoscience and Nanotechnology 11 (2011) 4923–4928.
[7] S. Kay, A. Thapa, K.M. Haberstroh, T.J. Webster, Tissue Engineering 8 (2002) 753–761.
[8] H.J. Lee, S.E. Kim, H.W. Choi, C.W. Kim, K.J. Kim, S.C. Lee, European Polymer Journal 43 (2007) 1602–1608.
[9] H.X. Diao, Y.F. Si, A.P. Zhu, L.J. Ji, H.C. Shi, Materials Science and Engineering: C 32 (2012) 1796–1801.
[10] A.S. Asran, S. Henning, G.H. Michler, Polymer 51 (2010) 68–876.
[11] F. Yang, J.G.C. Wolke, J.A. Jansen, Chemical Engineering Journal 137 (2008) 154–161.
[12] F.M. Zhang, J. Chang, J.X. Lu, C.Q. Ning, Materials Science and Engineering: C 28 (2008) 1330–1339.
[13] C. Harms, K. Helms, T. Taschner, I. Stratos, A. Ignatius, T. Gerber, S. Lenz, S. Rammelt, B. Vollmar, T. Mittlmeier, International Journal of Nanomedicine 7 (2012) 2883–2889.
[14] H. Kim, R.P. Camata, Y.K. Vohra, W.R. Lacefield, Journal of Materials Science Materials in Medicine 16 (2005) 961–966.
[15] W.G. Cui, X.H. Li, C.Y. Xie, J.G. Chen, J. Zou, S.B. Zhou, J. Weng, Polymer 51 (2010) 2320–2328.
[16] S.S. Kim, M. Sun Park, O. Jeon, C. Yong Choi, B.S. Kim, Biomaterials 27 (2006) 1399–1409.
[17] L. Borum-Nicholas Jr., O.C. Wilson, Biomaterials 24 (2003) 3671–3679.
[18] A.N. Hayati, S.M. Hosseinalipour, H.R. Rezaie, M.A. Shokrgozar, Materials Science and Engineering C 32 (2012) 416–422.
[19] X. Wang, G. Song, T. Lou, Medical Engineering and Physics 32 (2010) 391–397.
[20] W. Liu, Z.P. Xie, C. Jia, Journal of the European Ceramic Society 32 (2012) 1001–1006.
[21] X.F. Zhao, X.D. Li, Y.Q. Kang, Q. Yuan, International Journal of Nanomedicine 6 (2011) 1385–1390.
[22] C. Kunze, T. Freier, E. Helwig, B. Sandner, D. Reif, A. Wutzler, H.J. Radusch, Biomaterials 24 (2003) 967–974.
[23] J. Jagur-Grodzinski, Polymers for Advanced Technologies 17 (2006) 395–418.
[24] S. Drotleff, U. Lungwitz, M. Breunig, A. Dennis, T. Blunk, J. Tessmar, A. Göpferich, European Journal of Pharmaceutics and Biopharmaceutics 58 (2004) 385–407.
[25] P. Hariraksapitak, O. Suwantong, P. Pavasant, P. Supaphol, Polymer 49 (2008) 2678–2685.
[26] G. Guo, S.Z. Fu, L.X. Zhou, H. Liang, M. Fan, F. Luo, Z.Y. Qian, Y.Q. Wei, Nanoscale 3 (2011) 3825–3832.
[27] D.M. Zhang, A.P. Tong, L.X. Liang, F. Fang, G. Guo, Cytotechnology 64 (2012) 701–710.
[28] C.H. Chen, J.S. Peng, M. Chen, H.Y. Liu, C.J. Tsai, C.S. Yang, Colloid and Polymer Science 288 (2010) 731–738.
[29] M. Gigli, N. Lotti, M. Gazzano, L. Finelli, A. Munari, Polymer Engineering and Science 53 (2013) 491–501.
[30] Q.Y. Zhu, Y.S. He, J.B. Zeng, Q. Huang, Y.Z. Wang, Materials Chemistry and Physics 130 (2011) 943–949.
[31] H.S. Kim, H.J. Kim, J.W. Lee, I.G. Choi, Polymer Degradation and Stability 91 (2006) 1117–1127.
[32] H.Y. Li, J. Chang, A.M. Cao, J.Y. Wang, Macromolecular Bioscience 5 (2005) 433–440.
[33] J. Yang, W. Tian, Q. Li, Y. Li, A. Cao, Biomacromolecules 5 (2004) 2258–2268.
[34] J.M. Goddard, J.H. Hotchkiss, Progress in Polymer Science 32 (2007) 698–725.
[35] H.J. Lee, H.W. Choi, K.J. Kim, C.L. Lee, Chemistry of Materials 18 (2006) 5111–5118.
[36] X.Y. Li, K.H. Nan, S. Shi, H. Chen, International Journal of Biological Macromolecules 50 (2012) 43–49.
[37] Y. Ito, H. Hasuda, M. Kamitakahara, C. Ohtsuki, M. Tanihara, I.K. Kang, O.H. Kwon, Journal of Bioscience and Bioengineering 100 (2005) 43–49.
[38] A. Sionkowska, J. Kozłowska, International Journal of Biological Macromolecules 52 (2013) 250–259.
[39] H.E. Romeo, M.A. Fanovich, Journal of Materials Science Materials in Medicine 19 (2008) 2751–2760.
[40] K. Anselme, Biomaterials 21 (2000) 667–681.
[41] H.T. Sasmazel, International Journal of Biological Macromolecules 49 (2011) 838–846.